Hydrogen trapping in 3D-printed (additive manufactured) Ti-6Al-4V

Ravit Silverstein*, Dan Eliezer

Department of Materials Engineering, Ben-Gurion University of the Negev, Beer-Sheva, Israel

ARTICLE INFO

ABSTRACT

Hydrogen trapping state and desorption behavior in 3D printed-Ti-6Al-4V, designed using additive manufacturing (AM), have been investigated. The AM process in this work is selective laser melting (SLM) by which components are built using melting powder's layers with a laser beam. During this process, hydrogen can meet with Ti, leading to a catastrophically failure known as hydrogen embrittlement. The effect of hydrogen on different textural anisotropy of AM-Ti-6Al-4V, and on metal's defect (created during the SLM process), have been studied in relation with hydrogen trapping state, and hydrogen embrittlement. The common effect of hydrogen on phase transformation in AM-Ti-6Al-4V has been shown. It is shown that the susceptibility to hydrogen embrittlement significantly depends on the printing direction. The impact of hydrogen desorption on AM-Ti-6Al-4V have been demonstrated with thermal desorption spectrometry (TDS), X-ray diffraction (XRD) and microstructural observations.

1. Introduction

Titanium alloys offer a combination of attractive characters such as: high strength to weight ratio and good corrosion resistance [1]. These alloys are backbone materials in the aircraft industry, employed in all advanced gas turbine engines and advanced airframes for jet fighters. One of the favored compositions in the Ti industry is the Ti-6Al-4V, due to its unique crystal structure, of equiaxed α (hcp) and intergranular β (bcc), creating optimum mechanical properties [2,3]. Although titanium is considered to be reasonably resistant to chemical attack, severe problems can arise when titanium alloys come in contact with hydrogen. Hydrogen damage of titanium and its alloys is manifested as a loss of ductility (embrittlement) and/or reduction in the stress-intensity threshold for crack propagation. This phenomenon is known as hydrogen embrittlement [4,5].

The susceptibility to hydrogen embrittlement is directly related to the binding energy of hydrogen with the metal's defects, known as trapping sites. Since trapping affects control the availability of hydrogen to the critical cracking locations, it has a major influence on the hydrogen embrittlement phenomenon.

In recent times, the growing demand for producing complex-shaped functional metallic components, particularly Ti alloys, for aerospace, defense, and automotive industries has put into focus additive manufacturing (AM), and especially laser-based AM processes [6]. These processes have a complex non-equilibrium physical and chemical metallurgical nature, which is material and process-dependent [7]. One of the influences on AM processing is the interaction with hydrogen. The common processing and structures created during AM, such as: anisotropy and metal's defects, highly influence the metal's susceptibility to hydrogen embrittlement.

Therefore, a study of hydrogen–trapping interactions with Ti is crucial to predict its safe service conditions. Trapping characteristics are of great importance to determine whether a trap's binding energy has a strong connection to hydrogen to prevent it from reaching a cracking site.

In this work, different textures of SLM-Ti-6Al-4V parts will be investigated in regards to hydrogen interaction. The characteristics of hydrogen evolution hydrogen-trapping interactions were studied using thermal desorption spectrometry (TDS). This analysis is then used to assess the hydrogen evolution and trapping parameters within the context of the various microstructures of SLM-Ti-6Al-4V, and to explain the correlation between prior microstructure, hydrogen concentration, potential trapping states and the alloy's response to hydrogen embrittlement.

2. Experimental Procedure

2.1. Microstructure Analysis

Spherical powder of Ti-6Al-4V, produced by selective laser melting (SLM) technology, was investigated. Ti-6Al-4V parts were made of Ti-6Al-4V powder with particle size range between 20 and 65 μm using
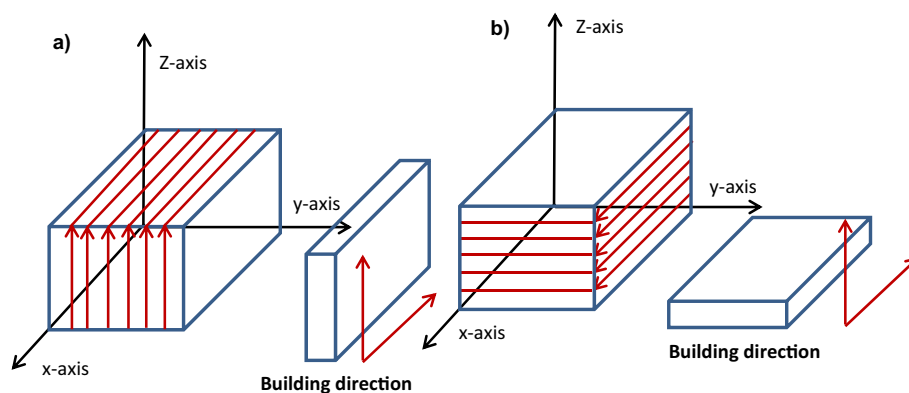

Fig. 1. Two different SLM-building directions: (a) SLM1 and (b) SLM2.

laser melting machine made by EOS (Electro Optical Systems), as can be seen in Fig. 1. In this work, the SLM installation was the EOSINT M 280 which is based on the innovative direct metal laser sintering. The EOSINT M 280 is equipped with SMYb:YAG-fibre laser with a maximum power of 400 W and a spot size of 80 μm. Samples were prepared with a scanning speed of 1000 mm/s, and 100 μm hatch spacing (distance between two adjacent scan vectors) [8]. The scanning direction was rotated 67° between consecutive layers to obtain optimal densification. Each sample was designed with a rectangular shape and printing orientation of ZX axis following the ISO/ASTM 52921-13 standard. The different building directions are designated as SLM 1 and SLM2 and can be seen in Fig. 1 a and Fig. 1 b, respectively.

Hydrogen interactions with SLM–Ti-6Al-4V were studied by exposing it to a gas-phase hydrogen charging. At this charging technique, the SLM–Ti-6Al-4V parts were exposed to 0.5 MPa hydrogen pressure at 500 °C for 10 h. With these charging conditions we aimed to create Ti-hydrides and homogeneous hydrogen content along the Ti bulk. Charging conditions were estimated according to the thin plate solution of Fick's second law [9], where the effective diffusion at 500 °C is D_{H_in} $_{Ti} \approx 1.02 \times 10^{-6}$ cm^2/s [10]. These charging conditions allowed for a homogenous content of ~100 wt% ppm along the sample bulk.

2.2. Thermal Desorption Spectrometry (TDS)

The characteristics of hydrogen desorption, and hydrogen trapping states were investigated by TDS. With this procedure, the desorption rate of hydrogen atoms is recorded while heating the sample a non-isothermal heating at a known rate under UHV conditions of ~10 MPa. In this work, samples were heated from RT to 500 °C at constant heating rates of 2 °C/min, 4 °C/min, and 6 °C/min. The thermo-desorption spectra is collected by the QMA 200 quadrupole mass-spectrometer under the fast multiple mode detection. The working procedure, as described elsewhere [11,12], allowed for the identification of different types of traps coexisting in the sample. The microstructure, phase composition, and lattice parameter were examined both– before and after the hydrogenation process by means of XRD. The XRD patterns were measured at RT with a Philips PW 1050/70 diffractometer using Ni-filtered Cu-Kα radiation (1.54 Å), scanned speed of 0.3°/min and 2θ range of 30–100°.

3. Results and Discussion

3.1. Microstructure of Different Textural Anisotropy AM–Ti-6Al-4V

The presented micrographs of AM–Ti-6Al-4V, Fig. 2 and Fig. 3, show a top and side view of different textural anisotropy. The different building directions are very well seen for both samples, Fig. 2 a and Fig. 3 a, for SLM1 and SLM2, respectively. The microstructure of both samples is consisted of acicular α (hcp microstructure) in the β

transformed phase (bcc microstructure) as can be well seen in Fig. 2 c and Fig. 3 b. The amount of each phase was calculated from XRD diffraction pattern, Fig. 4 and Fig. 5-as specified below, and predicted contents 60%–40% α-β-phases for each sample. Though they consist of the same powder size and have the same microstructure, the resulting morphology and metal's defects (due to different direction of building) show a major effect on the hydrogen embrittlement mechanism.

3.2. Microstructure Changes in the Presence of Hydrogen – Different AM Building Directions (SLM1 and SLM2)

The XRD diffraction patterns (Fig. 4 and Fig. 5) show a comparison between as-received AM- Ti-6Al-4V–SLM1 and Ti-6Al-4V–SLM2 and hydrogen charged (hydrogenated) after 1 week aging at room temperature (RT). Each sample (as-received-black line) consists of two phases: 60% acicular α (with hcp microstructure) and 40%-β transformed phase (bcc microstructure).

It can be seen, in both cases-red line, that Ti-α exhibit increased lattice parameter due to hydrogenation. This phenomenon has been considerably reviewed in the literature [13–16]. Hydrogen will generally lead to an increased lattice parameter [17–19]. If its solubility is high enough in specific phase then it can also form hydrides in some case. The higher content of hydrogen and lower solubility has led to additional reflections, which were ascribed to the precipitated δ-TiH$_x$ and γ*-TiH. The δ-TiH$_x$ precipitated has an fcc crystal lattice with hydrogen atoms occupying the tetrahedral interstitial sites- creating CaF$_2$; This non-stoichiometric structure exists over a range of 1.5 to 1.99 [20]. The γ*-TiH precipitated usually appears at low hydrogen concentrations (1–3 at.%), and has a tetragonal crystal structure with hydrogen atoms occupying one-half of the tetrahedral interstitial sites. Even though, the hydrogenated SLM samples, as shown in Fig. 4 and Fig. 5, present about the same behavior, there is a slight difference between the contents of Ti-hydrides. In order to asses those differences, phase's quantifications of δ-TiH$_x$ and γ*-TiH, α-Ti, and β-Ti were performed by the Rietveld refinement technique [21,22], which is based on phase's intensity difference. This procedure was already described in our previous works [17,19,23]. Using this method we could have estimated the quantities of Ti-hydrides. For the SLM1 sample, this method predicted contents of ~40% and ~18% of the whole sample for δ-TiH$_x$ and γ*-TiH, respectively. The calculation for SLM2 predicted ~25% and ~10% of the whole sample, for δ-TiH$_x$ and γ*-TiH, respectively. The differences in the hydrides amount can have a great impact on the hydrogen embrittlement mechanism, as we will see further on.

Micrographs of the sample's surface after the hydrogenated process can be seen in Fig. 6. Both hydrogenated samples, presented cracking on the surface. It can be seen from Fig. 6 a and Fig. 6 c, that the hydrogenated SLM1 sample revealed severe cracking compared with the hydrogenated SLM2 sample. These differences are probably related to the higher Ti-hydrides phases in SLM1 sample compared with SLM2.